Journal of Aeronautics, Astronautics and Aviation, Vol. 56, No. 1S, pp. 487 – 499(2024)
DOI: https://doi.org/10.6125/JoAAA.202403_56(1S).36

Self-Deployable Sail for CubeSat De-orbiting Mission: Preliminary Design and Demonstration of PANDORA

Syaril Azrad [1, 2 *] and Lit Yang Yeong [1]

[1] *Department of Aerospace Engineering, Faculty of Engineering, Universiti Putra Malaysia, 43400 Serdang, Selangor, Malaysia*
[2] *Aerospace Malaysia Research Center, Faculty of Engineering, Universiti Putra Malaysia 43400 UPM Serdang, Selangor, Malaysia*

ABSTRACT

Since the 1960s, the launching of satellites has increasingly caused the Earth's orbit to be filled with space debris travelling at very high speeds. To mitigate this problem, in 2007, the Inter-Agency Debris Coordination Committee (IADC) created a specific guideline to suggest every spacecraft, including satellites, to de-orbit itself within 25 years after the end of its mission within the Low Earth Orbit (LEO). CubeSat development and research can be cost-effective compared to larger satellite missions, making it the choice for many educational institutions to pursue space projects. However, the increasing number of CubeSat missions means that the issue of de-orbiting these microsatellites has become a pressing matter. This paper describes the design process, prototyping, and demonstration of a de-orbiting mechanism of a single-unit-size (1U) CubeSat using a passive sail membrane that is held in place by multiple booms, also named as PANDORA (Passive Sail Membrane Deployment Configuration). The multiple booms holding the thin film are released using a coil spring and Memory Alloy (SMA), which functions as a braking system, and it has been demonstrated that release took about 0.5 to 0.81 seconds. The materials used in the project are readily available and relatively low-cost considering the study, which serves as a proof of concept and is in its preliminary stage.

Keywords: CubeSat, Microsatellite, Space Debris, De-orbit Mechanism

I. INTRODUCTION

The increasing number of satellites in Low Earth Orbit (LEO) has amplified the need for effective de-orbiting strategies to mitigate the risk of space debris [1,7]. CubeSats, a class of research nanosatellites, have become a popular choice for space exploration and research due to their relatively low cost and compact size [2,5]. However, the cost of CubeSat projects can still be prohibitive for student-led initiatives, necessitating the exploration of cost-effective alternatives [2,8].

This paper presents a preliminary design and demonstration of a self-deployable sail for CubeSat de-orbiting missions. The project aims to bridge the gap between technical development and cost-effectiveness, focusing on a low-cost student project. The self-deployable sail is a promising solution for de-orbiting microsatellites, offering a cost-effective and technically feasible approach to managing space debris [3,6]. The concept of de-orbiting microsatellites involves using a drag sail to lower the satellite's altitude until it re-enters the Earth's atmosphere and burns up [3,6].

The use of self-deployable sails for de-orbiting microsatellites is indeed a promising solution for managing space debris. This approach is considered cost-effective and technically feasible, as evidenced by several missions and studies. The NanoSail-D2 mission conducted by NASA in 2011 effectively showcased the de-orbiting potential of a lightweight sail with a large surface area. In September 2011, the 3U spacecraft demonstrated its

Manuscript received, November 19, 2023, final revision, December 20, 2023
* To whom correspondence should be addressed, E-mail: syaril@upm.edu.my

capability for de-orbiting purposes by successfully re-entering Earth's atmosphere [9]. In 2017, the CanX-7 mission successfully implemented the deployment of a drag sail, providing additional evidence to support the viability of this particular methodology [9]. The Ultrasail project is a unique endeavour that integrates propulsion and control systems originally designed for formation-flying microsatellites with a novel solar sail architecture. This project is characterized by its high-risk nature and potential for significant rewards. The aforementioned system has the capability to attain controllable sail areas that are close to 1 km², hence presenting an unconventional method in the field of propulsion technology [10].

The HPS ADEO-L and ADEO-N represent instances of Deployable Drag-Sail De-Orbit sub-systems, which have been specifically engineered to cater to satellites of diverse dimensions. The sail areas of these systems can be customized based on the mass of the spacecraft and the desired de-orbit time (Source: [11]). Drag Augmentation Systems (DAS) refer to sails that are lightweight and cost-effective. These sails are deployed at the conclusion of a mission and serve as dependable solutions for de-orbiting tiny satellites. By facilitating the sustainable utilization of space, DAS contributes to the responsible management of space resources [12]. This method is particularly relevant for CubeSats, many of which do not carry a propulsion system that could otherwise assist in de-orbiting [7]. However, the high cost associated with CubeSat projects, particularly for student-led initiatives, presents a significant challenge [2,8].

In response to this challenge, this paper presents a low-cost, student-led project that demonstrates a preliminary design of a self-deployable sail for CubeSat de-orbiting missions. The project serves as a proof of concept, aiming to demonstrate that cost-effective and technically feasible solutions for de-orbiting microsatellites are within reach for student projects. The design and demonstration of the self-deployable sail are based on the utilization of commercial off-the-shelf components and low-thrust propulsion systems [4]. This paper will discuss the overall objectives and requirements of the CubeSat design in section 2. Section 3 describes the setup and methodology that has been adopted by the work. The results and discussion of the study are in section 4, while section 5 concludes the work with recommendations and future works.

II. DESIGN OBJECTIVES AND REQUIREMENTS

The primary aim of the study in this paper is to establish a preliminary design and to demonstrate a self-deployable sail for a 1U CubeSat using readily available low-cost materials and techniques. We have underlined the objectives as follows:

- To comprehensively research and evaluate available options and methodologies for developing a self-deployable sail design.
- To prototype a self-deployable sail design with the proof of concept in mind, using affordable materials readily available in the market.
- To focus on demonstrating the functionality and workability of the mechanical self-deployable sail design, emphasizing its manufacturability.

The overarching goal is to contribute to the advancement of satellite technology by introducing a reliable and cost-effective method for designing the mechanism for satellite de-orbiting through self-deployable sails.

2.1 Design Requirements

The design requirements for the self-deployable sail system are defined as follows:

(1) Able to passively de-orbit a 1U satellite in 550 km LEO in less than 25 years: The device's primary purpose is to facilitate the passive de-orbiting of a 1U satellite by utilizing aerodynamic drag generated from the sail's interaction with the residual atmosphere in Low Earth Orbit (LEO) [17]. At the end of the satellite's life, a small amount of energy is left to expense, and the mechanism must be activated with such minimum energy. This approach using sail ensures energy efficiency and mission completion within the designated 25-year timeframe, aligning with established guidelines such as the one underlined by the Inter-Agency Space Debris Coordination Committee (IADC) for spacecraft disposal [18]. A 550km altitude was selected as a case study as it is still considered within LEO, and many missions were launched to altitude due to its location in the sun-synchronous orbit. Examples of CubeSats released approximately between 500km to 550km are ANSER CubeSats, Passive Inspection CubeSats (PICs), Sateliot IoT and QB50 CubeSats. [13-16].

(2) The device must be within the size of a 1U satellite (100 mm x 100 mm x 100 mm). Careful consideration will be given to size constraints, with a commitment to ensuring that the device fits within the dimensions of a 1U CubeSat. Selective Laser Sintering (SLS) 3D printing may create lightweight and robust components. However, low-cost, off-the-shelf and readily available 3D printing materials are applied in this preliminary stage.

(3) Able to store and deploy a 1 M x 1 M Sail Membrane: In solar sail, the higher the ratio of sail size to the total mass of the satellite, the higher the values of characteristic acceleration of the solar sail [19,20]. The design must accommodate the storage and deployment of a 1 m x 1 m sail membrane to pave the way for larger or smaller sail configurations in future iterations. Additionally, the potential for the device to function as a solar sail, and thus its characteristic acceleration, will be explored to maximize performance.

(4) Motor-less deploying mechanism approach: A simple motor-less deployment mechanism to streamline the design by minimizing parts. This approach reduces costs and enhances the reliability and compactness of the device, increasing the likelihood of mission success.

(5) Contain fail-safe mechanisms to prevent the sail and booms from being accidentally deployed: Safety during all phases of the satellite mission is paramount.

A robust fail-safe mechanism will be integrated into the design to safeguard against unintentional deployment of the sail and its associated structural components. This precaution will account for the high-vibration conditions experienced during rocket launches and transportation into space, ensuring that the device remains securely stowed until intended deployment.

These defined requirements form the foundation of the design, guiding the development and testing of the self-deployable sail system for CubeSat missions. The subsequent sections of this paper will delve into the design and characterization of the sail system, addressing each requirement in detail.

III. SETUP AND METHODOLOGY

The flowchart of the entire process flow of the project is shown in Figure 1.

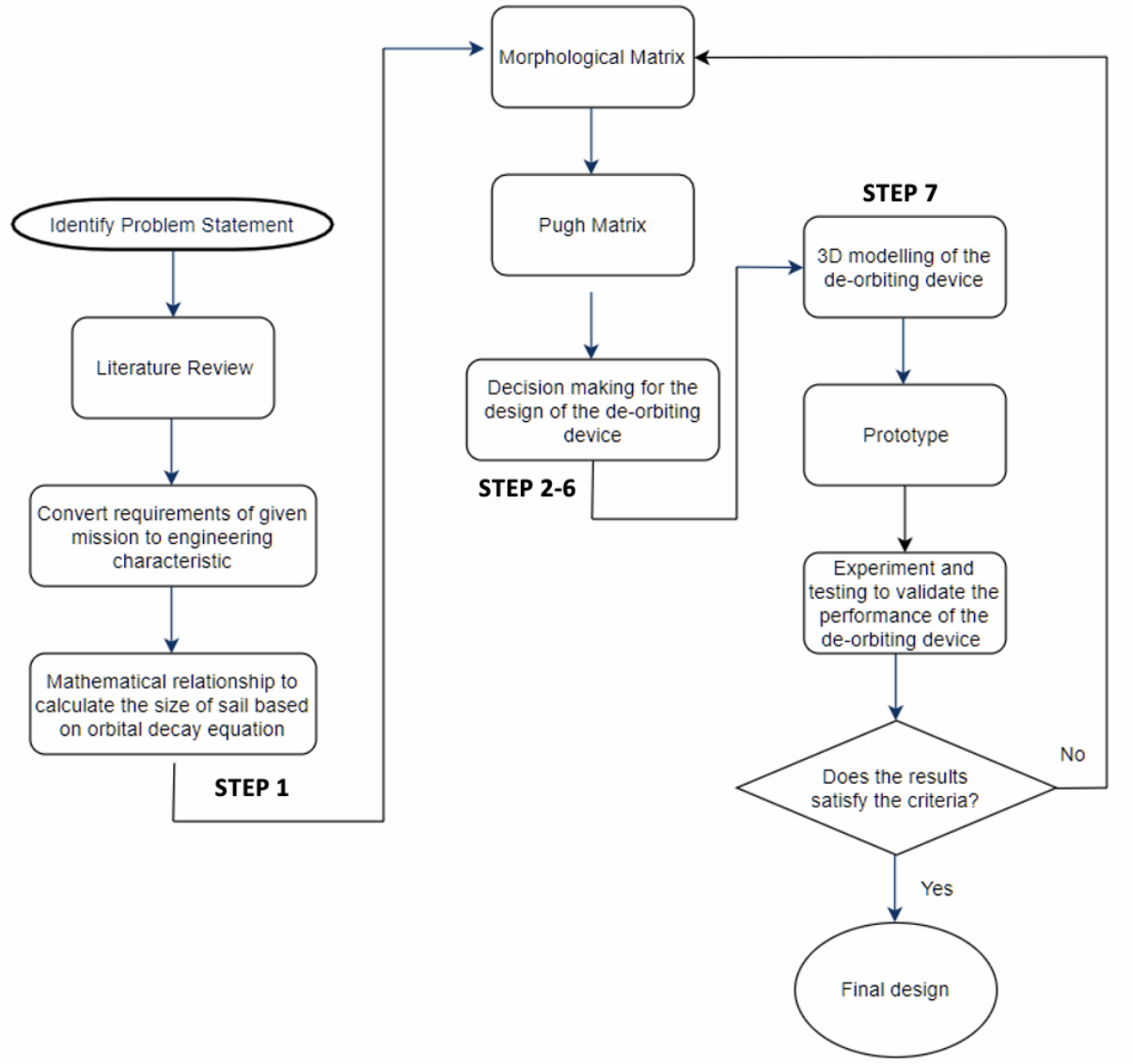

Figure 1 Flowchart for the entire design project

The steps that lead to the 3D modelling (**STEP 7**) and prototyping of the de-orbiting mechanism are listed below as **STEP 1** to **STEP 6**. The selection outcome is mentioned under each step listed below. However, note that before finalizing the design, a process of selection using a morphological matrix and Pugh matrix was utilized to decide the outcome of **STEP 2** to **STEP 6**. The morphological and Pugh matrix will be introduced in this paper after **STEP 7**.

STEP 1: Mathematical relationship to calculate the size of the sail

A small amount of atmospheric particles are still present in the LEO region. By utilizing these atmospheric particles, we can create an orbital decay using the atmospheric drag generated when the satellite collides with these particles. A drag sail can be used to decrease the amount of time needed to de-orbit the satellite to Earth after it has finished its mission. It will later burn up during re-entry due to the absence of high-temperature resistance

material [21]. To estimate the time required to de-orbit a 1U CubeSat using a certain sail size, first, we apply the Drag Force, F_D as shown in Equation (1):

$$F_D = \frac{1}{2}\rho V^2 A C_d \quad (1)$$

where ρ refers to air density, V is the velocity of the satellite relative to the fluid, A is the area exposed to the direction of motion and C_d is the coefficient of drag. The coefficient of drag is a constant value, and it depends on the shape of the satellite and how space particles collide with it. In this project, C_d is assumed to be 2.20, widely accepted and used as a standard in various works and models for a CubeSat in LEO. It was first developed as a mathematical construct by Cook [22] and later validated with theoretical laboratory work in gas-surface interactions such as Bird's [23]. We assume the satellite will have a circular orbit, and the relation between orbital period, P and semimajor axis, a can be expressed as follows:

$$P^2 GM = 4\pi^2 a^3, \text{ and } a = Re + H \quad (2)$$

where G is the gravity constant, M is the mass of Earth, Re is the radius of Earth, H is the starting altitude from the Then, the change in the period, dP due to atmospheric drag is given by Equation (3):

$$dP/dt = -3\pi a \rho (AC_d/m_{sat}) \quad (3)$$

where m_{sat} is the mass of the satellite, and dt is the change of time.

The mass of the 1U satellite is assumed to be 1.33 kg, with an additional 1 kg for the de-orbiter; the total weight of the satellite is now 2.33 kg. The area of the sail, A, set by the requirement, is 1m x 1m or 1.0 m^2 to calculate the performance of the aerodynamic drag and the change in altitude per day in kilometers. To determine the period change that can be used to calculate the change in altitude, we need to use an atmospheric model adapted from the Australian Space Weather Agency's model, which was derived using an empirical density model [24]. The model relates the density, ρ, at a certain altitude, h to the space environment through exospheric temperature, T. The temperature is specified as a function of the solar radio flux, $F10.7$, and the geomagnetic index Ap. The density is calculated using Equation (4):

$$\rho(h) = 6 \times 10^{10} exp\left(-\frac{h-175}{SH}\right) \quad (4)$$

with $SH = T/m_{atm}$ where $T = 900 + 2.5(F10.7 - 70) + 1.5Ap$ and $m_{atm} = 27 - 0.012(h - 20)$. Here, SH, is the variable scale height, and m_{atm}, is the effective atmospheric molecular mass. The results of the calculations of different altitudes are shown in Table 1.

In our calculation, the solar radio flux, $F10.7$, was set as 150 Solar Flux Units (SFU), and the geomagnetic index, Ap is 40. Re-entry is assumed to occur when the satellite has descended to an altitude of 180km. Since the requirement is to de-orbit a 1U satellite in 550 km LEO in less than 25 years, the 1 m x 1 m size of the drag sail will be sufficient for the mission as it takes no longer than 40 days to de-orbit from 550km LEO.

Table 1 Aerodynamic drag and change of altitude per day due to drag (1m x 1m), 1U

Initial Altitude (km)	Atmospheric Density (kg/m^3)	Time to De-orbit (days)	Change per day (km/day)
950	3.592 x 10^{-15}	6769	-0.120
850	8.434 x 10^{-15}	2434	-0.308
750	2.435 x 10^{-14}	730	-0.914
650	8.648 x 10^{-14}	183	-2.795
550	3.777 x 10^{-13}	40	-27.141
450	2.028 x 10^{-12}	8	-36.378
350	1.34 x 10^{-11}	2	-119.034

STEP 2: Decision-making on type of boom

Booms are deployable cantilever arms that extend from the main body of a satellite or spacecraft to perform various tasks. For microsatellites, there are several types of booms, including the TRAC (Triangular Rollable and Collapsible) boom [31], the BI-STEM (Storable Tubular Extendible Member) boom [32], the DCB (Deployable Composite Boom) [33] and the C Shape Boom (C Boom) [34]. Each of these booms has unique characteristics and applications.

In determining the appropriate boom for sail deployment, the sail's size, derived from mission-specific altitude and CubeSat dimensions (**STEP 1**), is pivotal. The boom's type directly influences its performance, especially when factoring in boom length, mission profile, and budgetary constraints. Optimal booms are both robust and lightweight.

For this study, readily available materials were prioritized over specialized ones. Measuring tapes, known for their durability and accessibility, are potential candidates. As proposed by V. Lappas et al. [25], a lenticular-shaped boom can be crafted by joining two measuring tapes with Kapton tape. While this design is resource-efficient, it's not without challenges. Common

measuring tapes are relatively thick, and combining two tapes exacerbates this. Increased thickness leads to a "bulging effect" due to shear load, compromising the boom's integrity and deployment predictability. While thinner custom-fabricated booms are an option, their production is both costly and outcome uncertain.

Considering the constraints, a tape spring-shaped boom is recommended. While a simple boom using bistable composite tape-springs presented in [26] configurations were considered, they consume excess space, potentially compromising sail membrane accommodation. Given the project's exploratory and low-cost nature, a tape spring shape proves adequate.

STEP 3: Decision-making on the boom deployment configuration

The satellite boom deployment configuration is a pivotal consideration that directly impacts the efficacy of the boom's deployment. Two primary configurations present themselves for such operations: the Tangential and the Radial deployment configurations. Each possesses inherent advantages and disadvantages, necessitating a detailed evaluation of the mission profile and the necessity for a motor during boom deployment to ascertain the optimal choice. Table 2 summarizes the reasons for selecting tangential deployment for this project.

Table 2 Selection criteria for boom deployment configuration: between tangential and radial deployment

Deployment Configuration	Reasons for Selection
Tangential Deployment	1. Allows for lower friction, reducing the risk of mechanical wear and tear. 2. Fewer moving parts in the core of the device, simplifying the design and potentially reducing the risk of mechanical failure. 3. It is less complicated to fold its sail membrane for storage and deployment purposes, which could be particularly beneficial in a motorless approach. 4. The tendency for the spring tape to return to its original shape is strong, making it a good reason to go motorless during deployment.
Radial Deployment	1.Reduces the transverse load onto the booms during deployment, potentially reducing the risk of damage. 2. Reduces mechanical shock at the root of the tape spring during the end of deployment, potentially reducing the risk of damage. 3. It is not suitable for this project due to the specific mission profile and the need for a motorless approach. 4. Often, it requires a motor to control the deployment, which could increase the total weight of the de-orbiter.

After delving into the specifics of the two deployment configurations, Tangential Deployment, characterized by reduced friction and fewer moving components at the device's core, emerges as the most fitting for this project. The configuration simplifies the process of folding the sail membrane for both storage and deployment. Nevertheless, a controlled speed during the boom's deployment is essential, mandating an external brake system.

STEP 4: Selection of the best folding method to store and deploy the sail membrane

The sail membrane plays a pivotal role in the de-orbiting device's functionality, being the primary component interacting with the thin atmospheric layer to decelerate the CubeSat, thus initiating de-orbiting procedures. Consequently, determining an efficient and effective method for its storage and deployment is paramount in the design process.

Given the preference for the tangential deployment method for the boom, several folding patterns emerge as strong contenders: the angled frog-leg folding pattern, circumferential umbrella folding pattern, Z-folding pattern, tree leaves folding pattern, and basic umbrella folding pattern.

The angled frog-leg folding pattern, as shown in Figure 2, has several advantages over other folding patterns, which make it a preferred choice for the de-orbiting sail deployment method for several reasons, namely (1) its ability to maximize packing efficiency, (2) its ability to minimize stress and simplify folding, (3) efficient for storage space, (4) compatible with tangential boom deployment mechanism and (5) its adaptability to different mission requirements [27].

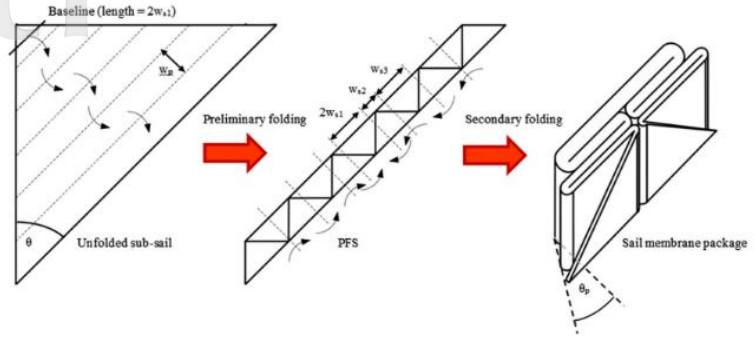

Figure 2 Angled frog-leg folding pattern [27]

STEP 5: Decision-making on the store location of the sail membrane

The optimal storage location for the sail membrane holds significant implications for the overall functionality of the de-orbiting device. It is imperative that the chosen location minimizes the risk of entanglement with other components during deployment. Such entanglements could hinder the membrane's deployment, jeopardizing the CubeSat's successful de-orbiting. Potential storage locations range from the device's exterior to its core, contingent on the de-orbiting device's design.

Two principal options present themselves for the sail membrane storage: atop the boom deployment mechanism or embedded within its center. For this design, positioning the sail membrane atop the boom deployment mechanism emerges as the superior choice. This separation minimizes the potential damage to the sail membrane during the prototyping phase. Moreover, available space atop the deployment mechanism ensures no constraints in accommodation. Crucially, this separation also curtails the likelihood of the boom and sail membrane becoming inadvertently intertwined during deployment.

STEP 6: Decision-making on the design of the brake mechanism

A braking system to regulate the deployment speed of the tape spring boom is necessary based on mission requirements. High-speed deployment may risk damaging the sail during deployment. This brake system remains modular, allowing for its attachment or detachment from the satellite.

A key component in the braking solution is the utilization of Shape Memory Alloy (SMA) to control the boom's deployment speed. This custom mechanism will regulate the core's rotational speed during deployment. Furthermore, the braking intensity is adjustable, driven by the electric current through the SMA, offering the ability to accelerate or decelerate deployment as needed.

STEP 7: 3D modelling of the de-orbit device

In response to the stipulated design requirements for the mission, a comprehensive three-dimensional model of the de-orbiting device was constructed. It is crucial to meticulously consider all design criteria and account for component modifications within the de-orbit mechanism. Before **STEP 7**, the design must be finalized using a selection process that applies morphology and the Pugh matrix. The actual 3D model of the de-orbiting device is shown in Figures 3 and Figure 4.

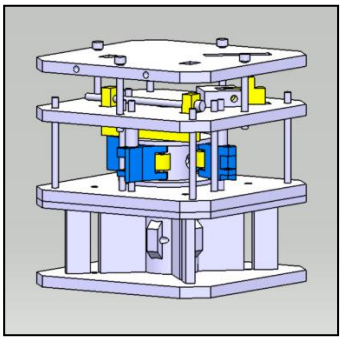

Figure 3 Assembled View

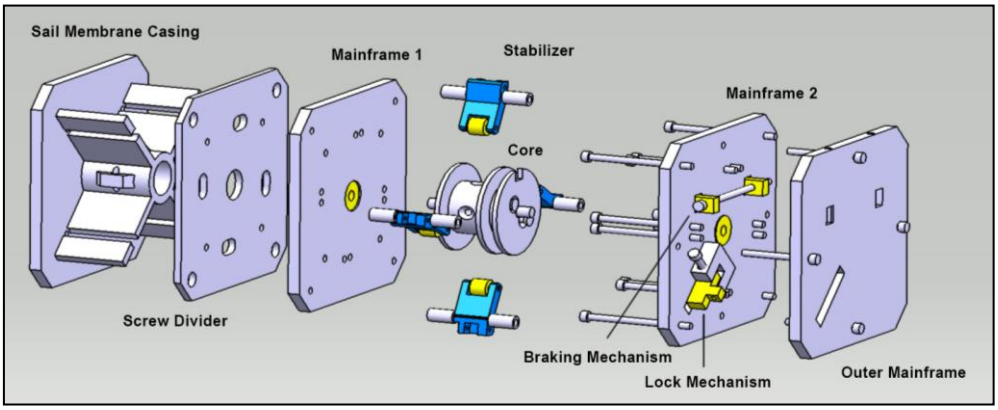

Figure 4 Explosion View

3.2 Design Decision Process

A design decision process using morphological and Pugh matrix has been applied in this work.

3.2.1 Morphological Matrix

Table 3 shows the morphological matrix that was created to generate ideas by combining several different combinations of possible designs for the project.

Table 3 Morphological Matrix Table

Parameter	Criteria 1	Criteria 2	Criteria 3	Criteria 4	Criteria 5
Type of Boom	C shape	TRAC	STEM	Bi STEM	C shape
Boom material	Tape spring	Stainless steel	Composite material	Composite material	Tape spring
Type of boom deployment mechanism	motorless	motor driven	motor driven	motor driven	motorless
Boom deployment configuration	Radial deployment configuration	Radial deployment configuration	Radial deployment configuration	Tangential deployment configuration	Tangential deployment configuration
Sail membrane material	Aluminized polyimide	Aluminum with Kapton	Aluminized polyimide	Aluminum with Kapton	Aluminum with Kapton
Folding Configuration	angled frog-leg folding pattern	circumferential umbrella folding	Z-fold	Rotationally skew folding	angled frog-leg folding pattern
Sail membrane storage location	middle	Top	middle	Bottom	Top

With the Morphological Matrix, as shown in the table, we can proceed and create a Pugh matrix to rate the best design for this project that suits the mission profile.

3.2.2 Pugh Matrix

From Table 4 and Table 5, it is shown that Criteria 5 or Design 5 have the highest value of them all. Criteria 1 was chosen to be used as the benchmark or reference for this Pugh matrix. All the different designs (Criteria 2 to 5) were compared with the reference design. When comparing, a -2, -1, 0, +1, +2 is used to state whether a concept is better or worse than the reference for a particular requirement. If it is better, a +1 or +2 is used; if worse, a -1 or -2, and if equal, 0. The primary requirements' total score is multiplied by 2, considering their influence on the final design selection.

Table 4 Pugh Matrix Table

Criteria	Criteria 1	Criteria 2	Criteria 3	Criteria 4	Criteria 5
Primary Requirement					
Size	0	-1	+1	+1	+1
Weight	0	-1	+1	+1	+2
Manufacturability	0	0	-1	+1	+1
Complexity	0	-1	-1	0	+1
Primary Total	0	-3	0	+3	+5
Secondary Requirement					
Cost	0	-2	-2	-2	0
Material Obtainability	0	-1	-2	-2	0
Numbers of moving parts	0	-1	0	-1	0
Secondary Total	0	-4	-4	-5	0

Table 5 Pugh Matrix Multiplier

Primary Total	0	-3	0	+3	+5
Primary Total (x2)	0	-6	0	+6	+10
Secondary Total	0	-4	-4	-5	0
Secondary Total (x1)	0	-4	-4	-5	0
Total	0	-10	-4	+1	+10

3.3 Prototyping of PANDORA

3.3.1 Material selection

For the screws in the device, stainless steel is the primary choice due to its superior resistance to corrosion. This ensures durability and consistency during the prototyping phase. In contrast, materials like iron would be susceptible to corrosion during standard testing, potentially leading to inconsistent results due to degradation.

The mainframes and other components not subjected to high temperatures are crafted from Polylactic Acid (PLA) plastic. PLA is favored for its ability to maintain accurate dimensions, even in larger print sizes. While Acrylonitrile Butadiene Styrene (ABS) plastic poses challenges in larger prints due to warping at the edges, it's advantageous for parts exposed to higher temperatures. This is particularly relevant in areas where the Shape Memory Alloy (SMA) is employed, as PLA could deform under such conditions. Therefore, ABS is utilized in these specific sections to withstand the heat produced by the SMA.

Lastly, a high-tension fishing line is integrated into the prototype for its strength and flexibility. It is especially crucial at the tape spring's tip, connecting the boom to the sail membrane and facilitating the boom's motion to deploy the sail. This robust line ensures that the device can handle the forces exerted during operations.

3.3.2 Core

The core serves as PANDORA's foundation, coordinating the boom, brakes, and lock mechanism. Critical to the device's function, any failure within the core jeopardizes the entire mechanism. Comprising four essential components – the main, middle, brake cores, and the thread linking to the mainframe – they interlock using two M3 13mm screws.

Though Aluminum 6061-T6 is the ideal material choice, this iteration, being a prototype, employs 3D printed PLA for demonstration. PLA offers ease of fabrication and sufficient mechanical strength. When assembling, it's crucial to eliminate any unevenness, preventing improper brake mechanism contact. Additionally, due to PLA's sensitivity to heat, storing the core below 60°C is advisable.

Throughout testing, the core performed as anticipated, proving the design's efficacy. Figure 5 shows the explosion, the assembled view, and the actual 3D-printed view of the core.

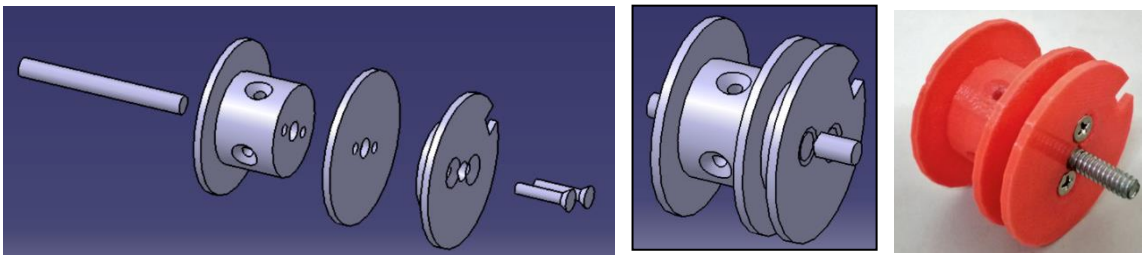

Explosion View Assembled View 3D Printed Core View

Figure 5 PANDORA Core View

3.3.3 Mainframe

Functioning as PANDORA's chassis, the mainframe secures all connections, facilitating mechanisms' actuation. Each device incorporates four distinct mainframes: those holding the SMA wire, those with the brake and lock mechanisms, those storing the sail membrane, and those that keep the sail membrane encased. The primary material envisaged for the mainframe was Aluminum 6061. However, for the prototyping phase, 3D printing using ABS and PLA proved adequate. Mainframes not exposed to high temperatures were crafted from PLA, while the SMA wire-bearing mainframe, which faces higher thermal conditions, was made of ABS.

Throughout evaluations, all four mainframes met expectations, sturdily maintaining component placement during the deployment processes.

3.3.4 Braking Mechanism

True to its name, this mechanism functions as the device's brake. Essential for motor-less sail deployment, the brake comprises two components: the brake and an M3 60mm screw. Various designs were considered, with a compact one eventually selected, albeit requiring further refinement to improve braking performance. The 3D-model view and the prototyped version are shown in Figure 6.

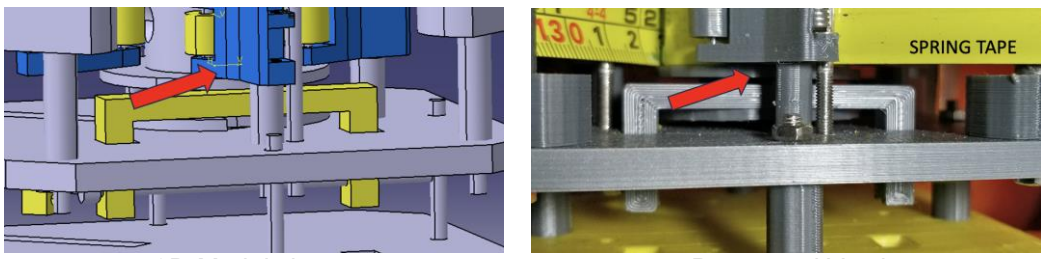

3D-Model view Prototyped Version

Figure 6 PANDORA Break Mechanism

3.3.5 Locking Mechanism

The locking mechanism, showcased in Figure 7, encompasses three components: a lock holder, the lock, and an M3 30mm screw. Once activated, the mechanism effectively restricts boom deployment. Nonetheless, questions about its reliability in unpredictable scenarios, such as during a rocket's launch vibrations or potential micro-meteorite impacts in Low Earth Orbit (LEO), remain.

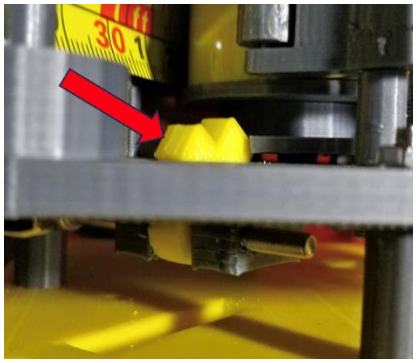

Figure 7 Prototyped Lock Mechanism

3.3.6 Roller

Figure 8 depicts a roller intended to minimize friction during boom deployment. For this prototype, the roller primarily guided the tape spring's direction rather than reducing friction.

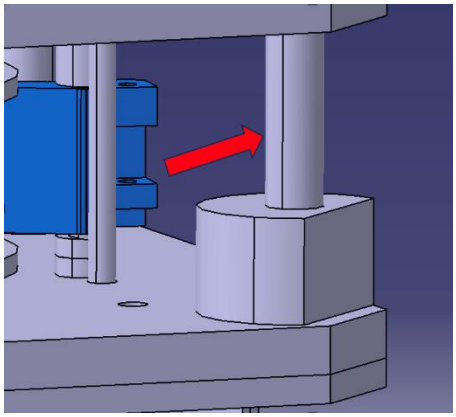

Figure 8 3D-Model of Roller Mechanism

3.3.7 Tape Spring

Each PANDORA has four tape springs anchored to the core using an M3 12mm screw.

3.3.8 Stabilizer

Stabilizers are crucial, ensuring effective tape spring deployment. Each core has four stabilizers, which significantly improved deployment smoothness during testing. Figures 9 and Figure 10 illustrate the stabilizers' arrangement within the device.

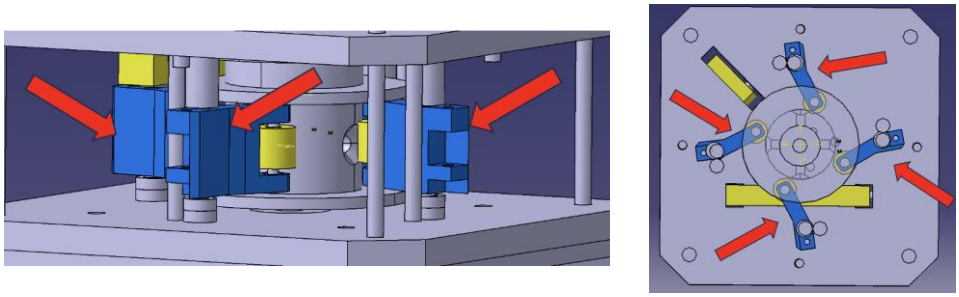

Figure 9 CAD Model of Stabilizers

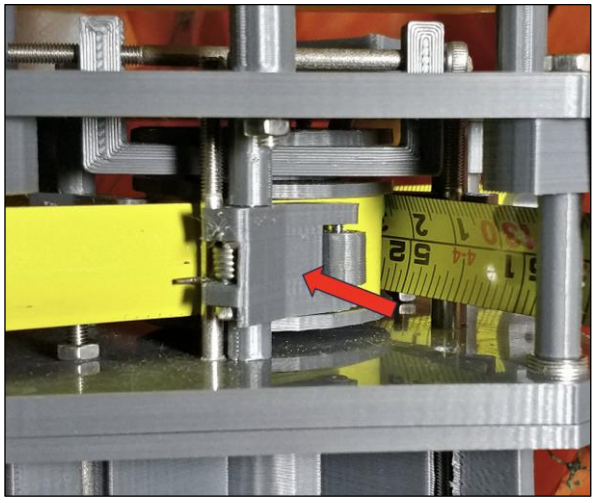

Figure 10 Prototyped 3D-printed Stabilize

3.3.9 Boom, Membrane Sail

The booms are made from 4 tape springs at a length of 0.7m as the aim of this project is to test out the concept of a 1m x 1m sail membrane deployment. Figure 11 shows the working final dimension of the sail and the boom.

While the specifics of an industrial-grade material remain non-essential at the prototype testing phase, a composite of Kapton tape and Aluminum foil serves as a viable substitute for the Aluminized Kapton Film [28]. The fabrication procedure involves trimming a standard kitchen-use aluminum foil to dimensions of 1m x 1m and subsequently overlaying it with a 50mm-wide Kapton tape. The resultant Kapton Tape Aluminum sail membrane closely resembles the industry standard Aluminized Kapton Film in appearance. Notably, the fabricated sail membrane exhibits greater thickness than the typical Aluminized Kapton Film, which can be custom designed to precise thicknesses, such as the 7µm mentioned in the works of Visagie and Fernandez et al. [29,30].

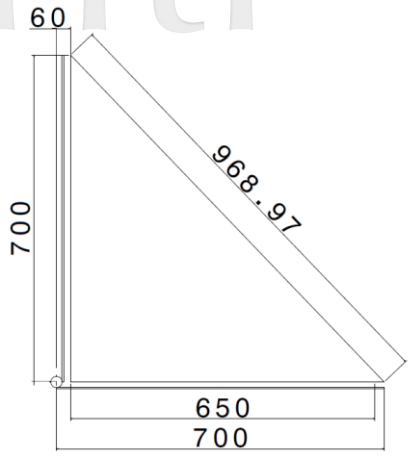

Figure 11 Dimension of the sail and boom

For preliminary deployment tests of the sail membrane, a synthetic cloth with a material thickness of 70µm is chosen for its durability, ensuring resilience across multiple test cycles. Figure 12 and Figure 13 show the unfolded aluminized Kapton sail membrane and a folded aluminized Kapton sail membrane using angled frog-leg folding pattern.

Figure 12 Aluminized Kapton Sail Membrane

Figure 13 Angled Frog-leg Folding Pattern

IV. RESULTS AND DISCUSSION

The brake mechanism and lock mechanism were tested using an external power supply to activate the SMA double helix and successfully released the boom, as shown in Figure 14. The reprogrammed SMA produced a force of 3.4N at the voltage of 2.5V and a current of 1.16A, which is the sufficient force needed to unlock the lock mechanism at 3.14N of PANDORA, allowing the release of the boom to deploy the sail membrane. This was using a single lock mechanism. A double lock mechanism was introduced with a voltage of 2.8V and a current of 1.28A to unlock a 6.28 N of lock force to ensure the reliability of the de-orbiter for the CubeSat.

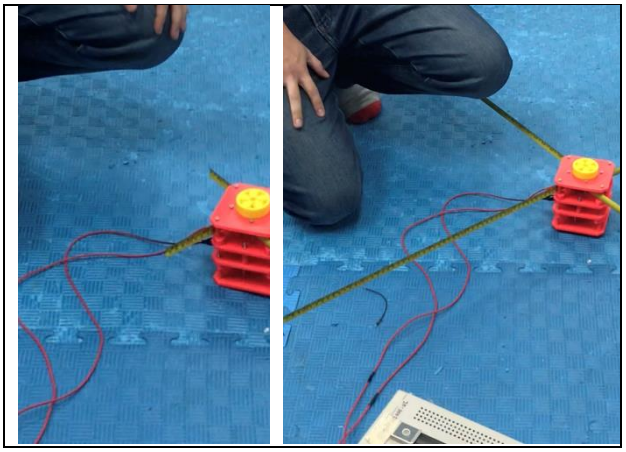

Figure 14 The boom was released approximately 0.5 seconds after the braking and locking were released

For the breaking mechanism, to reduce the speed of the boom deployment, the installed SMA does manage to slow down the deployment speed of the booms. However, for a controlled speed reduction of the booms during the deployment process, future work may be needed. The success rate of slowing down the deployment was inconsistent and is not reliable, with a 20% failure rate where the booms will not be deployed rather than slowing down. One method for controlling the boom deployment speed is to use a stepper motor on the PANDORA core. This will lead to extra weight, and a design selection process must be exercised.

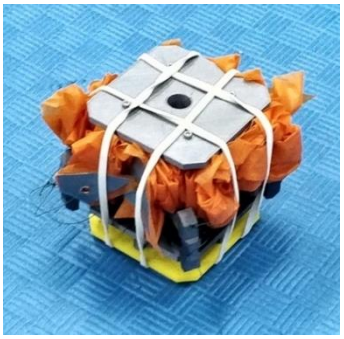

Figure 15 Ready-to-be-deployed PANDORA in preliminary demonstration

Figure 15 shows a ready-to-be-deployed PANDORA that demonstrates the deployment of the sail membrane of 1m x 1m. Instead of using the aluminized Kapton, we have decided to go with 70-micron thickness synthetic clothes that are much more versatile and will not tear easily during storage and deployment. By using the synthetic cloth, we managed to install it into the sail membrane compartment by using the frog-legged folding pattern. However, a few rubber bands were used to keep the sail membrane in the compartment as PANDORA was not installed with a sail membrane close lid to store the sail membrane

When it was ready to be deployed, the rubber bands were removed, and the release mechanism was activated. The release mechanism was activated by a string attached to the hole of the release mechanism to avoid the complexity of applying current to the installed SMAs. Figure 16 shows the sail membrane is being deployed successfully in the timeframe of less than a second, which is 0.81 seconds to be exact. Based on the results, the sail membrane deployment mechanism is a success and has functioned as intended.

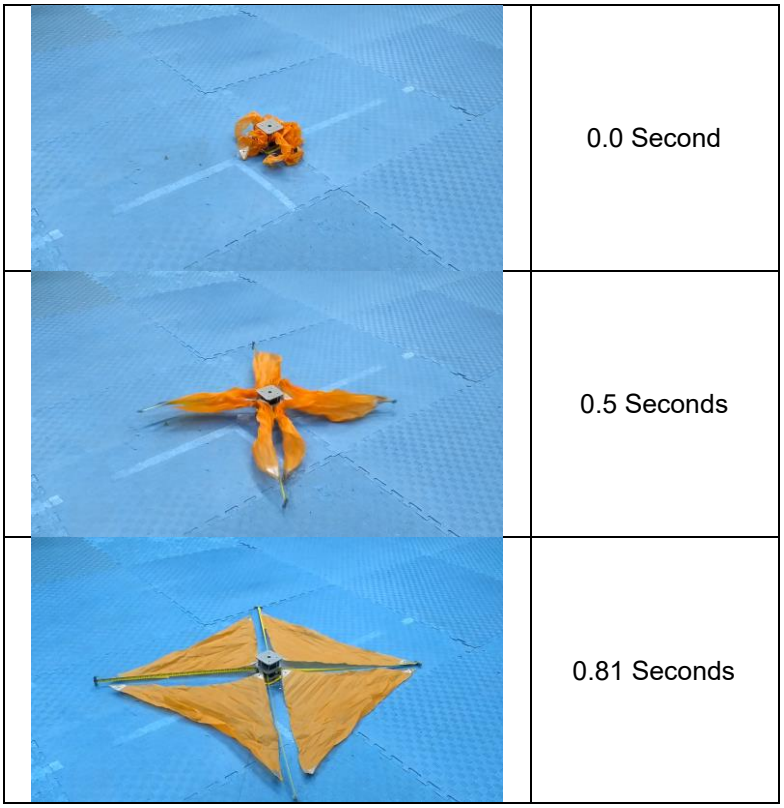

Figure 16 Deployment of PANDORA

V. CONCLUSIONS AND RECOMMENDATIONS

Based on our calculations, the de-orbiter is equipped to de-orbit a 1U CubeSat at a 550 km altitude within approximately 40 days. The prototype successfully deployed four tape spring booms, each 0.7 m in length, and a 1m x 1m sail membrane made of synthetic fabric. For successful boom deployment, four stabilizers were integrated near the core to prevent unwanted internal expansion. Comparative tests with and without these stabilizers revealed significant performance improvements with their inclusion. The NiTi Shape Memory Alloy was instrumental in the development of a braking mechanism and lock system to aid in the de-orbiter's deployment. While the current prototype's materials included 3D printed plastics such as PLA and ABS, future iterations anticipate the use of Aluminum 6061 T6. Ultimately, the project achieved all aims, objectives, and design requirements, demonstrating the successful development of a Self-Deployable Sail Design and Characterization for CubeSat Missions.

5.1 Recommendations

1. Boom Technology Advancement: Boom technology stands as a critical component in determining overall project success. Ensuring the boom is both robust and compact is paramount. Consideration of materials is crucial, with composite materials like carbon fibre suggested due to their customizability in size, fibre arrangement, and final form. Exploring other boom designs, such as STEM, BI-STEM, and TRAC, can also offer insights into performance enhancement. Dedicated research projects on this topic will be invaluable, fostering a deep understanding among engineers and students alike.

2. Deployment Mechanism Refinement: Although the Shape Memory Alloy (SMA) proves effective for the release mechanism, its efficacy as a braking system is sub-optimal. Motors, such as servo or stepper motors, may offer more precise deployment speed control by regulating the boom's release.
3. Integration of a Motherboard: The current project has validated the SMA, braking, and locking systems. Still, these components have yet to be tested in conjunction with a fully functional motherboard connected to batteries and a control station. Such integration would simulate LEO communication conditions, ensuring robust device command responsiveness. At this juncture, the Arduino Uno motherboard is recommended.
4. Sealable Lid Installation: Given PANDORA's utilization of a frog-legged folding configuration for the sail membrane, a sealable lid is necessary to prevent premature sail membrane deployment from its storage compartment. Either a motor or an SMA could control this lid, with a preference towards SMA due to its straightforward release mechanism.
5. Device Size Reduction: Having understood PANDORA's operational principles comprehensively, there is potential for significant device size reduction in future iterations. Given the notable thickness difference between the envisioned aluminized polyimide and the current synthetic fabric, there's a foreseeable decrease in the sail membrane compartment size.
6. Research on Sail Membrane Folding Patterns: The sail membrane's folding configuration offers abundant opportunities for research. By refining and experimenting with folding techniques, we can optimize PANDORA's overall dimensions while simultaneously minimizing deployment failures.

5.2 Future Works

It's imperative to consider testing the de-orbiter in varying environments, simulating the diverse conditions it might encounter in actual missions. Such tests can offer insights into unforeseen challenges, ensuring robust design adjustments in subsequent iterations.

ACKNOWLEDGMENTS

This work was supported by the Ministry of Education, Malaysia, through the Fundamental Research Grant Scheme (FRGS) under Grant FRGS/1/2020/TK0/UPM/02/33.

REFERENCES

[1] Takeda K, et al., "De-Orbit Maneuver Demonstration Results of Micro-Satellite ALE-1 with a Separable Drag Sail," *Applied Sciences*, Vol. 13, No. 13, Jun. 2023, p. 7737, doi: 10.3390/app13137737.

[2] Sato Y, Fujita S, Shibuya Y, Kuwahara T, Kamachi K, "In-orbit demonstration of reaction control System for Orbital Altitude Change of Micro-Satellite ALE-2", Proceedings of the Small Satellite Conference 2021 Technical Session 3 SSC21-III-09.

[3] "Aerospace." https://www.mdpi.com/journal/aerospace/special_issues/2319OV36DR (accessed Nov. 18, 2023).

[4] Hakima H, Emami MR, "Deorbiter CubeSat: Preliminary design and systems engineering budgets," in Proc. of the 68th International Astronautical Congress (IAC), Adelaide, Australia, Sep. 2017.

[5] "CubeSat Launch Initiative - NASA," NASA. https://www.nasa.gov/kennedy/launch-services-program/cubesat-launch-initiative/ (accessed Nov. 18, 2023).

[6] Nichols SJ, "De-orbiting drag sail," Doctoral dissertation, Naval Postgraduate School, Monterey, CA, 2020

[7] Pala A, Kuwahara T, Honda T, Uto H, Kaneko T, Potier A, Tangdhanakanond P, et al., "System Design, Development and Ground Verification of a Separable De-Orbit Mechanism for the Orbital Manoeuvre of Micro-Satellite ALE-1," *Transactions of the Japan Society for Aeronautical and Space Sciences, Aerospace Technology Japan*, Vol. 19, No. 3, 2021, pp. 360-367.

[8] "Small satellite projects," AeroSpace Ventures, Apr. 20, 2017. https://www.colorado.edu/aerospaceventures/what-we-do/small-satellite-projects (accessed Nov. 18, 2023).

[9] "13.0 De-orbit Systems - NASA," NASA. https://www.nasa.gov/smallsat-institute/sst-soa/deorbit-systems/

[10] Burton R, et al., "UltraSail - Ultra-Lightweight Solar Sail Concept," 41st AIAA/ASME/SAE/ASEE Joint Propulsion Conference & Exhibit. American Institute of Aeronautics and Astronautics, Jul. 10, 2005. doi: 10.2514/6.2005-4117

[11] Curtis H, "De-orbiting technologies for satellites: active and passive end-of-life systems on the global market," Satsearch Blog, Apr. 27, 2022. https://blog.satsearch.co/2022-04-14-de-orbiting-technologies-for-satellites-active-and-passive-end-of-life-systems-on-the-global-market

[12] Serfontein Z, Kingston J, Hobbs S, Holbrough IE, Beck JC, "Drag augmentation systems for space debris mitigation," *Acta Astronautica*, Vol. 188. Elsevier BV, pp. 278-288, Nov. 2021. doi: 10.1016/j.actaastro.2021.05.038.

[13] S. X, "Vega's fuel-free CubeSats will use wings to keep in formation," https://phys.org/news/2023-09-vega-fuel-free-cubesats-wings-formation.html, Sep. 27, 2023. [Online]. Available: https://phys.org/news/2023-09-vega-fuel-free-cubesats-wings-formation.html

[14] "Passive Inspection Cubesats," Spacecraft. https://spacecraft.byu.edu/missions/pics/ (accessed Nov. 18, 2023).

[15] "Sateliot IoT - EOPortal," Dec. 06, 2022. https://www.eoportal.org/satellite-

missions/sateliot-iot#eop-quick-facts-section (accessed Nov. 18, 2023).

[16] Caspi A, et al., "Small satellite mission concepts for space weather research and as pathfinders for operations," *Space Weather-the International Journal of Research and Applications*, Vol. 20, No. 2, Jan. 2022, doi: 10.1029/2020sw002554.

[17] Visagie L, Lappas V, Erb S, "Drag sails for space debris mitigation," *Acta Astronaut*., Vol. 109, 2015, pp. 65-75.

[18] Inter-Agency Space Debris Coordination Committee, "IADC Space Debris Mitigation Guidelines (IADC-02-01 Revision 1)," No. October, 2002, pp. 1-10.

[19] Costanza G, Leoncini G, Quadrini F, Tata ME, "Design and Characterization of a Small-Scale Solar Sail Prototype by Integrating NiTi SMA and Carbon Fibre Composite," *Advances in Materials Science and Engineering*, Vol. 2017.

[20] Sokolowski W, Tan S, Willis P, Pryor M, "Shape memory self-deployable structures for solar sails," No. December 2008, p. 72670K, 2008.

[21] Andrews J, Watry K, Brown K, "Nanosat De-orbit and Recovery System to Enable New Missions," 25th Annual AIAA/USU Conference on Small Satellites, 2011, pp. 1-5.

[22] Cook G, "Satellite drag coefficients," Planetary and Space Science, Vol. 13, No. 10, 1965, pp. 929-946.

[23] Bird GA, "Molecular gas dynamics and the direct simulation of gas flows," Oxford University Press, 1994

[24] Kennwell J, Panwar R, "Satellite Orbital Decay Calculations," Australian Space Weather Agency, 1999

[25] Lappas V, et al., "CubeSail: A low-cost CubeSat based solar sail demonstration mission," *Advances in Space Research*, Vol. 48, No. 11, 2011, pp. 1890-1901.

[26] Costantine J, Tawk Y, Christodoulou CG, Banik J, Lane S, "Cubesat deployable antenna using bistable composite tape-springs," *IEEE Antennas and Wireless Propagation Letters*, Vol. 11, 2012, pp. 285-288.

[27] Harkness P, McRobb M, Lützkendorf P, Milligan R, Feeney A, Clark C, "Development status of AEOLDOS - A de-orbit module for small satellites," *Advances in Space Research*, Vol. 54, No. 1, 2014, pp. 82-91.

[28] Dahl M, et al., "Design and Characterization of a Small-Scale Solar Sail Prototype by Integrating NiTi SMA and Carbon Fibre Composite," *Advances in Space Research*, Vol. 54, No. 1, 2015, p. 72670K.

[29] Visagie L, Lappas V, Erb S, "Drag sails for space debris mitigation," *Acta Astronautica*, Vol. 109, 2015, pp. 65-75.

[30] Fernandez JM, et al., "Design and development of a gossamer sail system for de-orbiting in low earth orbit," *Acta Astronautica,* Vol. 103, 2014, pp. 204-225.

[31] Leclerc C, Pellegrino S, "Ultra-thin composite deployable booms," in Proceedings of IASS Annual Symposia, International Association for Shell and Spatial Structures (IASS), 2017.

[32] Herlem F, 'Modelling and manufacturing of a composite bi-stable boom for small satellites,' 2014.

[33] NASA, "Deployable Composite Booms (DCB) - NASA," NASA, Jul. 26, 2023. https://www.nasa.gov/centers-and-facilities/langley/deployable-composite-booms-dcb/ (accessed Nov. 19, 2023).

[34] Barbera D, Laurenzi S, "Nonlinear buckling and folding analysis of a storable tubular ultrathin boom for nanosatellites," *Composite Structures*, Vol. 132, Nov. 2015, pp. 226-238, doi: 10.1016/j.compstruct.2015.05.024